SUPPLEMENTARY MATERIAL

Flavonoid compounds and antibacterial mechanisms of different parts of white guava (*Psidium guajava* L. cv. Pearl)

Wanjun Zhang[a], Jingyi Wang[a], Yashu Chen[a], Hongbin Zheng[a], Bijun Xie[a] and Zhida Sun[a,*]

[a]Natural Product Laboratory, Department of Food Science and Technology, Huazhong Agricultural University, Wuhan, Hubei 430070, People's Republic of China

*Correspondence should be addressed to Zhida Sun at the following addresses:

Mailing address: Department of Food Science and Technology, Huazhong Agricultural University, Wuhan 430070, People's Republic of China

*Telephone: +86-27-87283201. Fax: +86-27-87282966.

*E-mail: sunzhida@sina.com

Abstract: The flavonoid compositions, extracted from leaves, peel and flesh of white guava (*Psidium guajava* L. cv. Pearl), were identified and quantified by UPLC-ESI-QTOF-MS, HPLC-ESI-MS/MS and HPLC. The main components of three extracts all were quercetin-glycosides, but the proportion and content of quercetin-hexoside and quercetin-pentoside in each extract were different. Based on the measurements of MIC, MBC value and time killing curve, it emerged that 3 flavonoid extracts of white guava had good antibacterial effects on four pathogenic bacteria. White guava leaves flavonoids (WGLF) concentrations of 5.00 mg/mL and 0.625 mg/mL could change the micro-morphology of *Escherichia coli* and *Staphylococcus aureus*. It suggested that the antibacterial mechanism of WGLF on gram-positive and gram-negative bacteria was to destroy the structure and function of the cell membrane. It is indicated that the flavonoid extracts from white guava is a potential natural antimicrobial agent.

Keywords: *Psidium guajava* L.; Flavonoid compounds; UPLC-ESI-QTOF-MS; HPLC-ESI-MS/MS; Antibacterial activity; Antibacterial mechanism

1 Experimental

1.1 Chemicals and materials

All reagents and solvents used in this research were of analytical or HPLC grade. Methanol and acetonitrile were obtained from Sigma-Aldrich (St. Louis, MO, USA). Formic acid and the standards (quercetin, quercetin-3-*O*-glucoside and quercetin-3-*O*-arabinopyranoside) were purchased from Shanghai Yuanye Bio-technology Co., Ltd. (Shanghai, China) and water was Milli-Q quality. Luria Bertani broth (LBB), Luria Bertani agar (LBA), Mueller Hinton broth (MHB) and Mueller Hinton agar (MHA) were purchased from Hope Bio-technology (Qingdao, China). Four different microorganisms were obtained from China General Microbiological Culture Collection center (CGMCC), including *Escherichia coli* (25922), S*taphylococcus aureus* (26085), *Salmonella enterica* (50335) and *Shigella flexneri* (51574).

Fresh white guava (*Psidium guajava* L. cv. Pearl) leaves, fruit and red guava (*Psidium guajava* L. cv. Ruby) leaves were collected from Guangzhou in June 2017, and their voucher specimen numbers were PGL-20170604-013, PGF-20170604-021 and RGL-20170604-008 respectively. Plant variety was verified by researcher Li Chunyu, Institute of Fruit Tree Research, GuangDong academy of Agricultural Science.

Guava leaves were air-dried at 25°C until they reached constant weight, ground, and sieved (60 mesh) before analyses. The peel and flesh were kept in cold (-20°C) dark storage until processing.

1.2 Preparation of plant extract

Extraction method of total flavonoids from white guava was as follows: 1g dried, powdered white guava leaves were extracted with 10 mL ethanol/water=7/3 (V/V) at 60°C for 2 h. 1g fresh weight, peel and flesh of white guava was extracted with 3 mL ethanol/water=8/2 (V/V) at 50°C for 2.5 h. Three kinds of crude flavonoids aqueous solution were loaded onto an AB-8 resin column, and the fraction eluted by 50%, 80% and 80% ethanol was collected respectively. The eluant was evaporated at 40°C, and the white guava leaves flavonoids (WGLF), white guava peel flavonoids (WGPF) and whitel guava flesh flavonoids (WGFF) were obtained. Red guava leaves flavonoids (RGLF) were obtained using the same process as WGLF.

1.3 Determination of flavonoids purity

The flavonoids purity was determined as previously reported (Xie et al. 2015) with a modification. Briefly, 3.5 mL of 70% ethanol was mixed with 0.5 mL of the sample extract and 0.25 mL of 5% $NaNO_2$. After 5 min, 0.25 mL of 10% $Al(NO)_3$ solution was added and kept for 5 min. Then, 1.5 mL of 4% NaOH was added. The absorbance was measured after 15 min at 510 nm. The total flavonoid contents (%) were calculated using calibration curves of rutin.

1.4 Flavonoid composition analyses

1.4.1 Quantification of major flavonoid compounds

Quantification analyses of four flavonoid extracts (WGLF, WGPF, WGFF and RGLF) were performed on an HPLC system (Waters, America) and a GS-120-5-C18-A column (250 × 4.6, 5 μm) was equipped. The mobile phases were 0.1% formic acid water (A) and acetonitrile (B). Gradient elution conditions were as follows: a linear gradient with 5% B for 5 min, 15% B at 10 min, 25% B at 35 min, and 55% B from 45 to 50 min. The injection volume and flow rate were 10 μL and 1.0 mL/min, respectively. According to the peak area, quercetin-3-*O*-glucoside, quercetin-3-*O*-arabinopyranoside and quercetin were used to calculate the content of quercetin-hexoside, quercetin-pentoside and quercetin in samples, respectively. The results were expressed as μg of each flavonoid compound per mg of the sample (μg/mg).

1.4.2 Identification of flavonoid compounds

HPLC - ESI - MS/MS analyses. The above HPLC system was coupled to a Agilent 1100 Series LC-MSD-Trap-XCT to contrast the difference of WGLF with RGLF. An ESI ion source type in the negative mode was set with following parameters setting: capillary voltage: 350 V, corona voltage: 1.0 V and atomizing chamber voltage:10 psi; the ion source temperature and atomizing chamber temperature were 300°C and 350°C, respectively. The scan range was from m/z 100 to 1000 (Flores et al. 2015).

UPLC - ESI - QTOF - MS analyses. The further identification of flavonoids in leaves, peel and flesh of white guava (WGLF, WGPF and WGFF) were carried out in an Acquity UPLC system (Waters, Milford, MA, USA), and a BEH Shield RP18 column (100 mm × 2.1 mm, 1.7 μm) was equipped (Rojas-Garbanzo et al. 2016). The mobile phases were 0.1% formic acid water (A) and acetonitrile (B). Gradient elution conditions were as follows: a linear gradient with 2% B for 0 min, 50% B at 28 min, 100% B from 28.5 min to 30.5 min, and 2% B from 32 to 34 min, at a flow rate of 0.3 mL/min, The injection volume was 1 μL, and the column temperature was 35°C. The scan range was from m/z 100 to 1000. The source temperature was 150°C with a cone gas (nitrogen) flow 50 L/h, and the desolvation temperature was 450°C with a desolvation gas (nitrogen) flow 800 L/h. Electrospray voltageo was set at 1 kV for ESI ion source type in negative mode with the cone voltage at 40 V.

1.5 Antibacterial activity assay

1.5.1 Bacterial strain and culture conditions

Four bacterial strains were stored at -80°C in 30% glycerol stocks, and each of the bacterial strains were sub-cultured on LBA for two times. Before experiments, the single colony of four bacterial strains was cultured 6-8 h in LBB (200 rpm) to obtain the cells in an exponential period of growth. Then, the bacteria were centrifuged (7000 g, 5 min), washed twice, and suspended in 0.9% sterile saline. The turbidity of cell suspensions was determined by using McFarland standard.

15.2 Determination of Minimum inhibitory concentrations (MIC) and minimum bactericidal concentrations

(MBC)

The MIC and MBC of 3 flavonoids (WGLF, WGPF and WGFF) were tested by macro broth dilution method according to Chinese Medical Association Standards (CLSI 2012). The turbidity of the inoculum was adjusted to 0.5 McFarland standards and further diluted with MHB to achieve approximately 10^6 CFU/mL. Three kinds of flavonoids dissolved in sterile saline, 100 μL sample solution and 100 μL MHB were added to 96-well plates, and each sample was diluted to eight gradients by a double dilution method so that its concentration range was 0.0781-10 mg/mL. After that, 100 μL bacteria solution was added and incubated at 37°C for 24 h. Wells were assessed visually: the lowest concentration of the drug in the wells without bacteria growth was the MIC of the tested bacteria, the MBC was obtained by sub-culturing the test dilution on to MHA and incubated further (Gullon et al. 2016). All these assays were performed in triplicate, and penicillin was used as the positive control.

1.5.3 Time-kill assay

Time-kill curves were used to study the effect of antimicrobial agent concentration on bacterial growth in 96-well plates over time. Three samples were dissolved into 10 mg/mL with sterile saline. In the 96-well plates, 100 μL of sample solution and 100 μL of MH medium were added. Each sample was further diluted to eight gradients by the method of two-fold dilution, another 100 μL bacteria (10^6 CFU/mL) liquid was added to make the final volume of each hole to be 200 μL afterwards. The sample control group was replaced by MH medium, and the negative control medium was substituted for the sample solution. Plates were incubated at 37°C and the optical density was measured every two hours. All these assays were performed in triplicate, and penicillin was used as the positive control.

1.6 Antibacterial mechanism

1.6.1 Leakage of Potassium Ions

The extracellular potassium content was determined by flame atomic absorption spectroscopy method (Roosild et al. 2010). The cell suspensions of *E. coli* and *S. aureus* were treated with WGLF at different concentration and incubated at 37°C. The final bacterial cell concentration was approximately 10^8 CFU/mL. Samples (3 mL) of cell suspension were collected at various time intervals of 5, 15, 30, 60, 90, 120, and 150 min and were centrifuged at 7000 g for 5 min, the supernatant was sampled and diluted at 2-fold to determine the extracellular potassium content. A series of concentrations of potassium standard solution was prepared to generate a calibration curve, which was used to measure the leakage amount of potassium ion after the sample acting on the bacteria.

1.6.2 Leakage of proteins

The release of proteins from *E. coli* and *S. aureus* were measured by Coomassie brilliant blue method (Wang et al. 2015). Leakage of proteins through membrane of *E. coli* and *S. aureus* cells (10^8 CFU/mL)

were measured after 2, 4, 6, 8, 10 and 12 h exposure to WGLF with three concentrations. The suspensions were sampled and centrifuged (7000 g, 5 min) to determine the leakage of proteins. Stocked bovine serum albumin solution as a standard substance was prepared to obtain the calibration curve. All the samples were measured by determining the absorbance at 595 nm and the protein content was expressed in the light of the standard curve.

1.6.3 Flow cytometry method

The damage effect of WGLF on membrane permeability of *E. coli* and *S. aureus* was evaluated by determining the staining rate of bacterial cells infected with propidium iodide (PI) (Tang et al. 2017). The cells suspension (10^8 CFU/mL) of two bacteria were treated with different concentrations of WGLF and incubated at 37°C for 10, 20 and 40min. The cells were harvested by centrifugation (7000 g, 5 min), washed twice with sterile saline and dyed by PI (10 μg/mL) for 30 minutes in a dark place. The cell suspensions were then washed and examined by FACSCalibur flow cytometer (US BD Company).

Scanning electron microscopy (SEM) and transmission electron microscopy (TEM) analyses

Before SEM and TEM analyses, the cell suspension of *E. coli* and *S. aureus* (10^8 CFU/mL) were respectively incubated with 2MIC and MIC concentration of WGLF for 12 h at 37°C (Liu et al. 2016).

The micro-morphological changes of *E. coli* and *S. aureus* with or without WGLF treatment were observed by SEM (Xiong et al. 2017). The bacterial cells were harvested by centrifugation (7000 g, 5min), washed twice with sterile saline, and fixed in 2.5% glutaralde for 4 h. Then the bacterial samples were dehydrated in ethanol with a gradient of concentration (30%, 50%, 70%). After vacuum freeze drying, the samples were coated with gold and observed with scanning electron microscope.

On the basis of scanning electron microscopic analyzing was used to observe changes in the intracellular organization of *E. coli* and *S. aureus* with or without WGLF. The bacterial cells were harvested and dehydrated as described above, and then stained with sodium phosphotungstate. Finally, the bacteria were examined under transmission electron microscopy.

1.7 Statistical analyses

Statistical analyses were reported as mean ± standard deviation. All data set comparisons were made using One-way variance test and Tukey (ANOVA) test to analyse the significant differences among samples at $p < 0.05$. Spass 18.0 (IBM company; Armonk, NY) and Origin 8.0 (OriginLab company; Northampton, MA) were used for the statistical analyses.

2 Result supplement

Guava has many bioactive compounds. The flesh of guava mainly contains 3-caryophyllene, nerolidol and 3-phenylpropyl, while ascorbic acid is the main constituent of the guava peel. In addition, guava leaves contain essential oil, flavonoids, guayavolic acids, triterpenic acids and tannin (Gutiérrez et al. 2008).

According to recent reports, Venditti and Ukwueze (2017) found a glycosidic benzophenone substance in guava leaves which could completely replace the B ring, and Wen Ouyang et al. (2016) obtained two novel skeletal sesquiterpenoids in guava leaves guavacid A and isocaryolan-9-one, respectively**.** Recently, flavonoids have been widely concerned for their excellent biological activity. Therefore, this study focused on the analysis of flavonoids, and explored the differences in the composition and content of flavonoids in leaves, peel and pulp of guava.

2.1 Qualitative analyses of flavonoid compounds in 3 parts of white guava

UPLC-ESI-QTOF-MS was used to analyses the flavonoids that were extracted from three part of white guava (Table S1). Quercetin with an excimer ion peak $[M-H]^-$ at m/z 301.0337 was confirmed to exist in WGPF with a retention time of 15.503 min, and two typical fragments of quercetin at m/z 178.9949 and 151.0014 were detected in the secondary mass spectra of the ion at m/z 301.0337. Quercetin-hexoside was detected in WGLF and WGPF. For example, this compound in WGLF shown the excimer ion peak $[M-H]^-$ at m/z 463.0778 and the main fragment at m/z 301.0323 corresponding to loss of the hexoside moiety (162.0455 Da). Similarly, there are three peaks in the negative electrospray mass spectrum results of WGLF, WGPF and WGFF could be identified as quercetin-pentoside. Quercetin-pentoside in WGLF had a ion $[M-H]^-$ at m/z 433.0775 showed the fragments at m/z 300.0339 responding to losses of 133.0436 Da (pentoside moiety) from a quercetin backbone (Ming-Zhi et al. 2015).There a compound was tentatively assigned epicatechin because it presented the excimer ion peak $[M-H]^-$ at m/z of 289.0699. Moreover, four fragments ions at m/z 125.0415 (C ring 1, 4 bond fracture), 179.0320 $[M-C_6H_6O_2]^-$, 205.0452 $[M-2C_2H_2O]^-$ and 245.0788 $[M-CO_2]^-$were detected in the secondary mass spectra of the excimer ion at m/z 289.0699 (Chen et al. 2018). We could conclude that epicatechin was contained in WGLF, WGPF and WGFF.

The isolated of WGLF, WGPF, WGFF were characterized by HPLC (Fig S1), and the compounds in WGLF were further identified by HPLC - ESI - MS/MS (Table S3). Peak 1 produced a $[M-H]^-$ ion at m/z 476.9 and a characteristic ion at m/z 300.7 corresponding to losses of 176.2 Da (glucuronide moiety). Peak 1 was tentatively assigned as quercetin-glucuronide (Schieber et al. 2015). Quercetin and its glucosides (hexoside and pentoside) could be identified (the fragment pathways of these fragment ion was the same as *UPLC-ESI-QTOF-MS analyses*). In addition, three reference specimens were also analyzed by HPLC-ESI-MS/MS. According to the MS data (Table S2 and S3) and the elution result of reference specimens (Fig S1), peak 2 could be determined as quercetin-3-*O*-glucoside, peak 4 could be identified as quercetin-3-*O*-arabinopyranoside (guajaverin) and peak 6 could be identified as quercetin. Peak 7, which was the only one peak existed in WGFF, could not be determined at present and needed further analyses.

2.2 Quantitative analyses of major flavonoid compounds in three part of white guava.

In order to express the relative proportion of quercetin and its glycosides in those three flavonoids (WGLF, WGPF and WGFF), the peak area percentage were shown in Table S4. The sum peak area (%) of quercetin and its glycosides respectively occupied 90.8, 73.76, 0 of total peak area of WGLF, WGPF and WGFF. The ratio of quercetin-hexoside and quercetin-pentoside in WGLF, WGPF were nearly 1:5, 1:14, respectively. Moreover, quercetin-hexoside and quercetin-pentoside was quantified by comparing the samples with reference specimen (Table S5). The content of quercetin-hexoside in WGLF (9.27±0.036 μg/mg) was more than 13 times that of WGPF, and the content of quercetin-pentoside (56.17±0.058 μg/mg) in WGLF was more than 5 times that of WGPF. On the whole, the content of quercetin and its glucosides in WGLF (65.45±0.072 μg/mg) was significantly higher than WGPF and WGFF.

2.3 Comparison of flavonoid components in leaves of white and red guava.

The differences in flavonoid compounds between RGLF and WGLF were qualitatively and quantitatively analysed. The peaks 2 to 5 were all detected in WGLF and RGLF, and peak 1 as quercetin-glucuronide was unique to WGLF. The flavonoids in WGLF was dominated by quercetin-pentoside with the highest content of quercetin-3-*O*-arabinopyranoside (39.71±0.073 μg/mg), while RGLF was mainly composed of quercetin-hexoside identified as Quercetin-3-*O*-glucoside (15.04±0.025 μg/mg).

Table S1. Mass date of flavonoid compounds in leaves, peel and flesh of white guava (*P.guajava* L. cv. Pearl).

Compound	RT (min)	m/z $[M–H]^-$	Error (ppm)	Ion fragment	Identity	Formula
1	6.870_L[a]	289.0699	-4.2	125.0415,179.0320,205.0452, 245.0788	Epicatechin	$C_{15}H_{14}O_6$
	6.895_P[b]	289.0701	-4.2	125.0415,179.0320,205.0452, 245.0788		
	6.958_F[c]	289.0696	-5.5	125.0220, 137.0226, 245.0785		
2	15.503_P	301.0337	3.7	151.0009, 178.9949	Quercetin	$C_{15}H_{10}O_7$
3	10.960_L	463.0888	0.6	301.0329,271.0239,178.9961, 151.0007	Quercetin-hexoside	$C_{21}H_{20}O_{12}$
	11.190_L	463.0778	2.4	301.0323, 271.0239, 151.0007		
	11.050_P	463.0879	0.4	301.0331, 271.0327, 151.0019		
	11.275_P	463.088	0.6	301.0326, 271.0227		
4	11.665_L	433.077	0.9	301.0239, 178.9950, 151.0004	Quercetin-pentoside	$C_{20}H_{18}O_{11}$
	11.812_L	433.0775	1.2	301.0264, 178.9934, 151.0006		
	12.049_L	433.0775	2.1	301.0391, 151.0004		
	11.686_P	433.0772	0.2	301.0266,178.9950,271.0226, 151.0031		
	11.885_P	433.0767	0	301.0258,178.9934,271.0231, 151.0003		
	12.138_P	433.0761	-2.3	301.0254, 178.9957, 271.0226, 151.0003		
	11.679_F	433.0751	-4.6	178.8490, 151.0390		
	11.917_F	433.0728	-9.9	178.8368, 151.0006, 121.028		
	12.154_F	433.0736	-3.5	178.8356		

[a] RT_L, retention time in white guava leaves flavonoids (WGLF)

[b] RT_P, retention time in white guava peel flavonoids (WGPF)

[c] RT_F, retention time in white guava flesh flavonoids (WGFF)

Table S2. Mass date of three kinds of reference specimens.

Reference specimens	RT(min)	$[M–H]^-$	Ion fragment
Quercetin-3-*O*-glucoside	30.1	462.8	150.7, 178.6, 300.7
Quercetin-3-*O*-arabinopyranoside	34.3	433.0	178.6, 300.6
Quercetin	45.2	300.6	150.7, 178.7

RT: retention time

Table S3. Mass date of flavonoid compounds in leaves of white and red guava.

Peak number	RT(min)	$[M–H]^-$	Ion fragment	Identification
1	29.8_L	476.9	300.8	Quercetin-glucuronide
2	30.7_L	462.8	150.7, 300.6	Quercetin-3-*O*-glucoside
	30.4_{RL}	462.9	150.8, 300.7	
3	33.1_L	433.1	300.7	Quercetin-pentoside
	33.2_{RL}	433.0	300.6	
4	34.4_L	433.0	300.7, 178.7	Quercetin-3-*O*-arabinopyranoside
	34.5_{RL}	433.1	300.7	
5	35.0_L	433.1	300.7	Quercetin-pentoside
	35.0_{RL}	433.1	300.7	

RT_L, retention time in white guava leaves flavonoids (WGLF)

RT_{RL}, retention time in red guava leaves flavonoids (RGLF)

Table S4. Peak (%) of each component in four flavonoids.

Peak	RGLF	WGLF	WGPF	WGFF
	Area %	Area %	Area %	Area %
1		9.2	20.78	
2	83.35	14.81	4.9	
3	5.45	4.42	9.04	
4	5.58	53.7	11.01	
5	5.62	17.87	40	
6			8.81	
7				94.46
other quercetin and its glycosides	100	90.8	5.46 73.76	5.54 0

Table S5. The contents of quercetin hexoside, quercetin-pentoside and quercetin in samples were calculated by standard flavonoids according to the peak area by HPLC.

Samples	Quercetin-hexoside (μg/mg)	Quercetin-pentoside (μg/mg)	Quercetin (μg/mg)
RGLF	15.04±0.025	5.00±0.009	ND
WGLF	9.27±0.036	56.17±0.058	ND
WGPF	0.69±0.002	10.09±0.012	0.79±0.004
WGFF	ND	ND	ND

ND: not detected

Table S6. The minimum inhibitory concentration (MIC) and minimum bactericidal concentration (MBC) of WGLF, WGPF and WGFF against four pathogenic bacteria.

WGLF		WGPF		WGFF		penicillin	
MIC (mg/mL)	MBC (mg/mL)	MIC (mg/mL)	MBC (mg/mL)	MIC (mg/mL)	MBC (mg/mL)	MIC (mg/mL)	MBC (mg/mL)
2.5	5	2.5	5	5	10	<0.0781	<0.0781
0.313	0.313	0.313	0.625	0.625	1.25	<0.0781	<0.0781
1.25	5	2.5	5	5	10	<0.0781	<0.0781
2.5	5	5	5	5	10	<0.0781	<0.0781

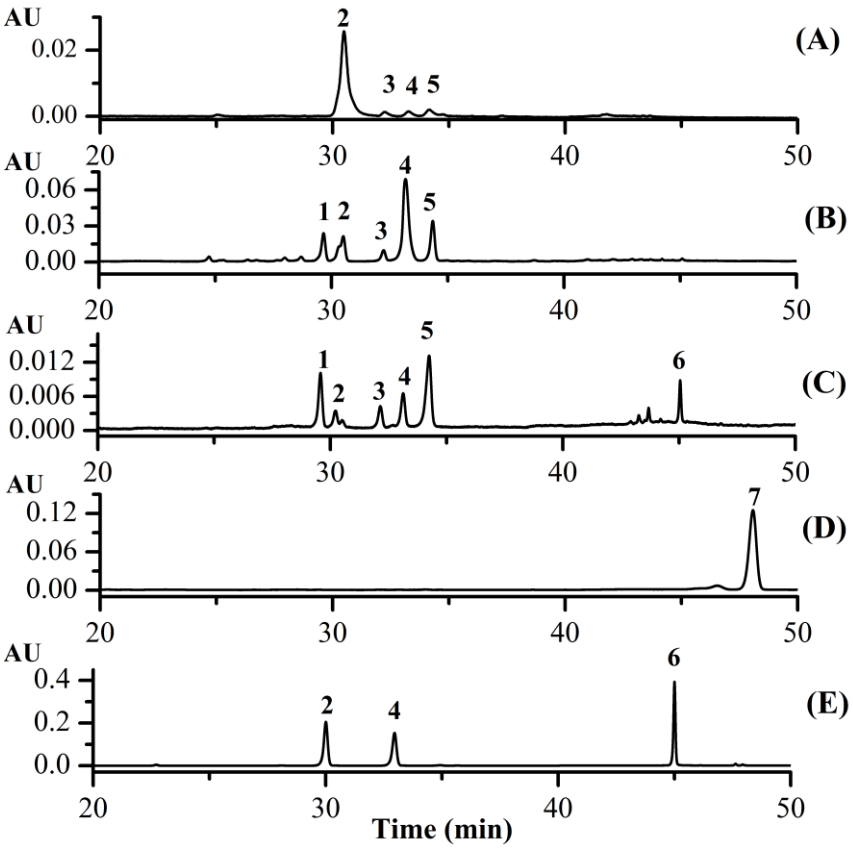

Fig S1. HPLC profiles analyses at 350 nm of (a) RGLF, (b) WGLF, (c) WGPF, (d) WGFF and (e) reference specimens: 2. quercetin-3-*O*-glucoside; 4. quercetin-3-*O*-arabinopyranoside; 6. quercetin.

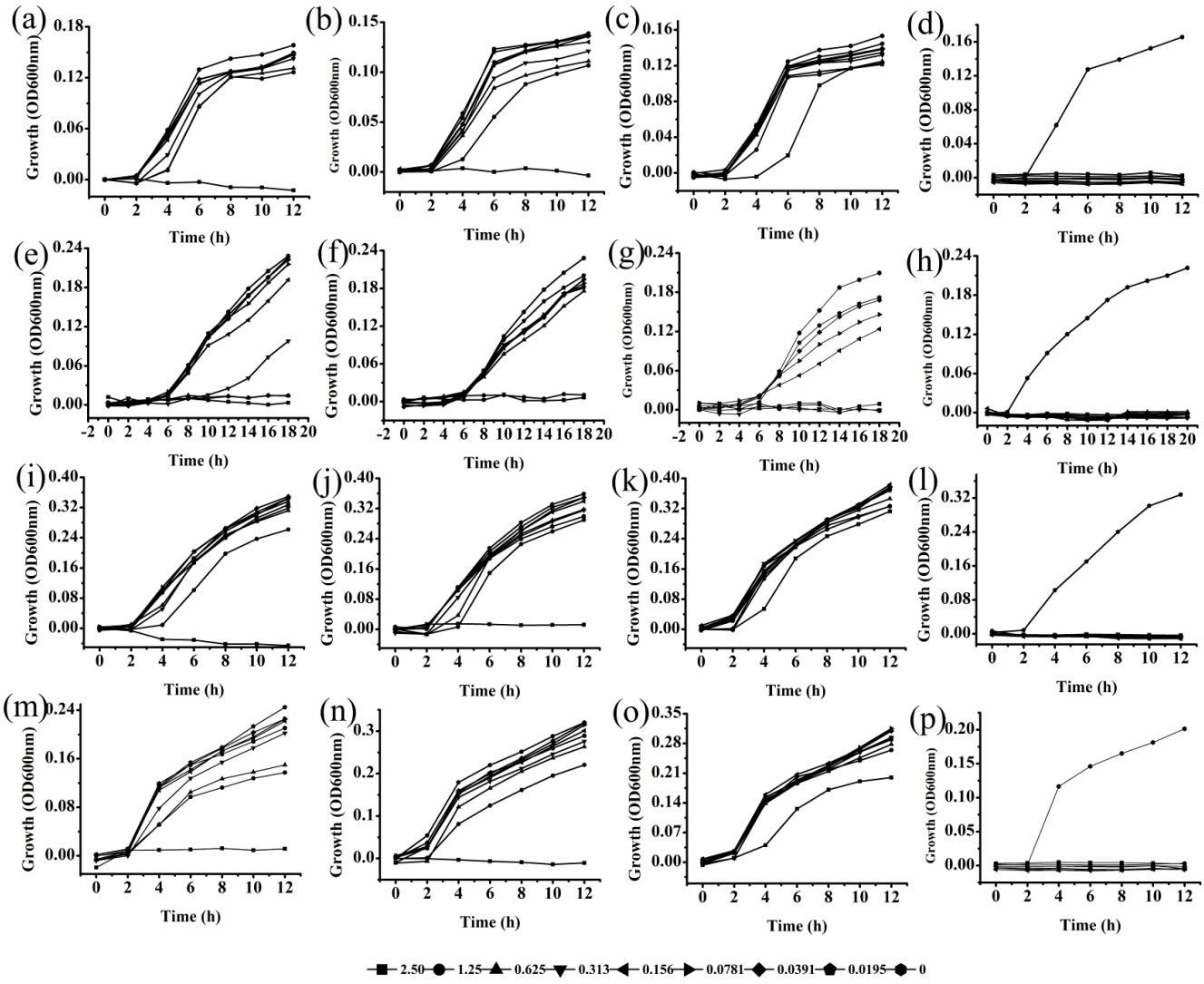

Fig S2. Time–kill curves of WGLF, WGPF, WGFF and penicillin respectively against four pathogenic bacteria (a, b, c, d) *E. coli*, (e, f, g, h) *S. aureus*, (i, j, k, l) *Salmonella* and (m, n, o, p) *Shigella*.

The bacterial growth kinetics showed that the growth inhibition rate of *E. coli* and *S. aureus* gradually increased until the inhibition rate reached 100%. However, the three samples have low doses to promote high dose inhibition of the growth of *Salmonella* and *Shigella*. For the above results, the conversion concentration range of WGLF on *Salmonella* and *Shigella* was the same: 0.156-0.313 mg/mL. Furthermore, the conversion concentration range of WGPF on *Salmonella* and *Shigella* was 0.625-1.25 mg/mL and 0.156-0.313 mg/mL, respectively.

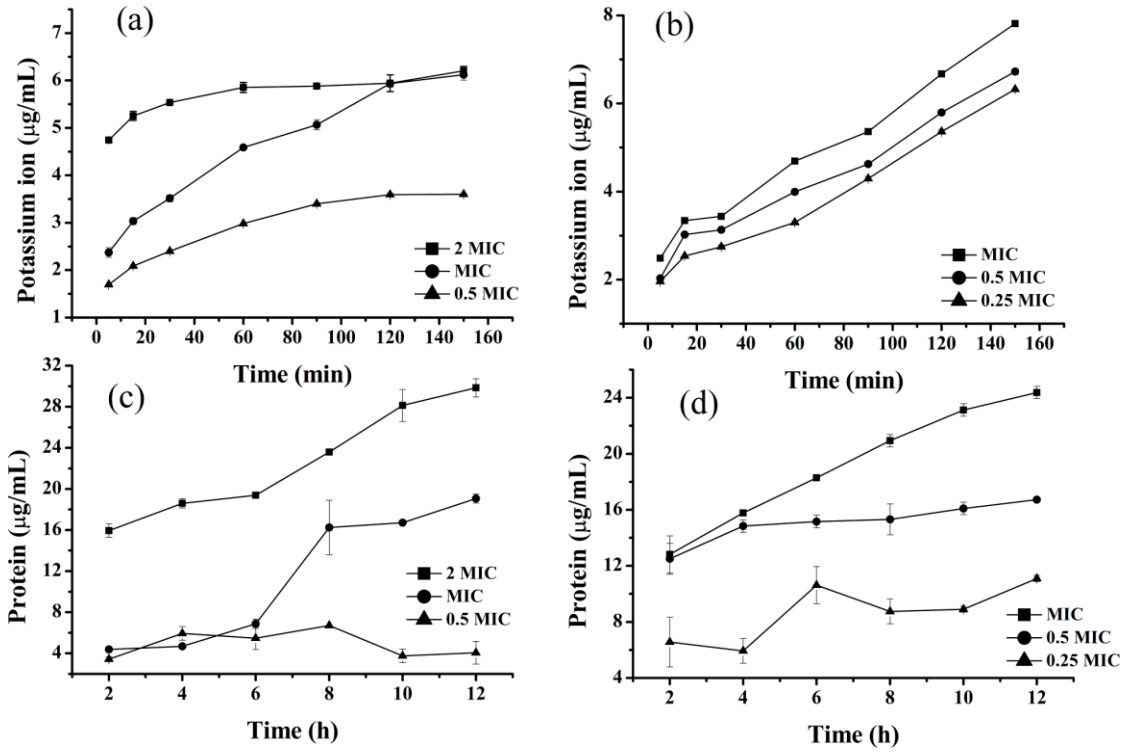

Fig S3. Potassium ion and Protein level in (a, c) *E. coli* and (b, d) *S. aureus* cell after incubation with WGLF.

Perumal et al. (2017) investigated the bacteriostatic mechanism of caffic Acid and Epicatechin 3-gallate in *Euphorbia hirta*. The authors suggested that bacterial cell membranes had many important functions, such as transport, respiration and lipid synthesis, and suggested that flavonoids can induce pore formation and lead to leakage of intracellular components, leading to cell death. In this study, the cells of *E. coli* and *S. aureus* treated by WGLF showed large leakages of potassium ions and proteins essential for maintaining several important cellular functions. This indicated that WGLF could change the permeability of bacterial membranes, leading to severe membrane damage and cell death.

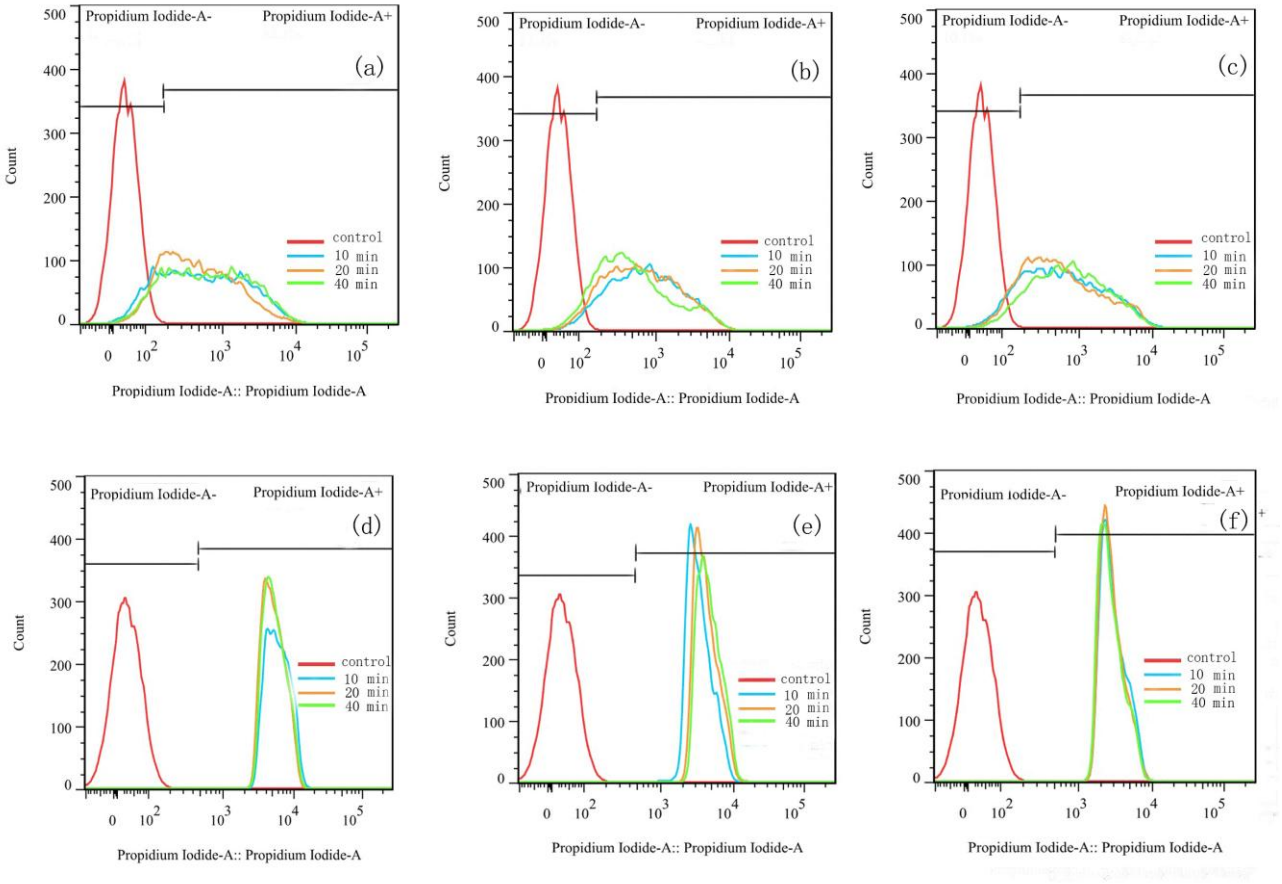

Fig S4. Flow cytometric analyses of *E. coli* and *S. aureus* cell suspensions after 10, 20, 40 min incubation with WGLF. (a, b, c) the PI staining rate of *E. coli* treated by WGLF with 0.5MIC, MIC and 2MIC.(d, e, f) the PI staining rate of *S aureus* treated by WGLF with 0.25MIC, 0.5MIC and MIC.

In this study, the untreated cells did not have PI fluorescence signal. However, a large proportion of *E. coli* and *S. aureus* cells were stained by PI after treating with WGLF. This observation is consistent with the finding of Sharma and Srivastava (2014). The authors showed that the membrane integrity of bacterial cells treated with an effective drug would be destroyed, allowing the PI dye to bind to the nucleus of the cell to produce fluorescence. Therefore, we could use the damage effect of drug on the integrity of pathogenic bacteria cell membrane as an indicator to show its antibacterial effect. WGLF had used this mode of action to achieve the bacteriostatic effect.

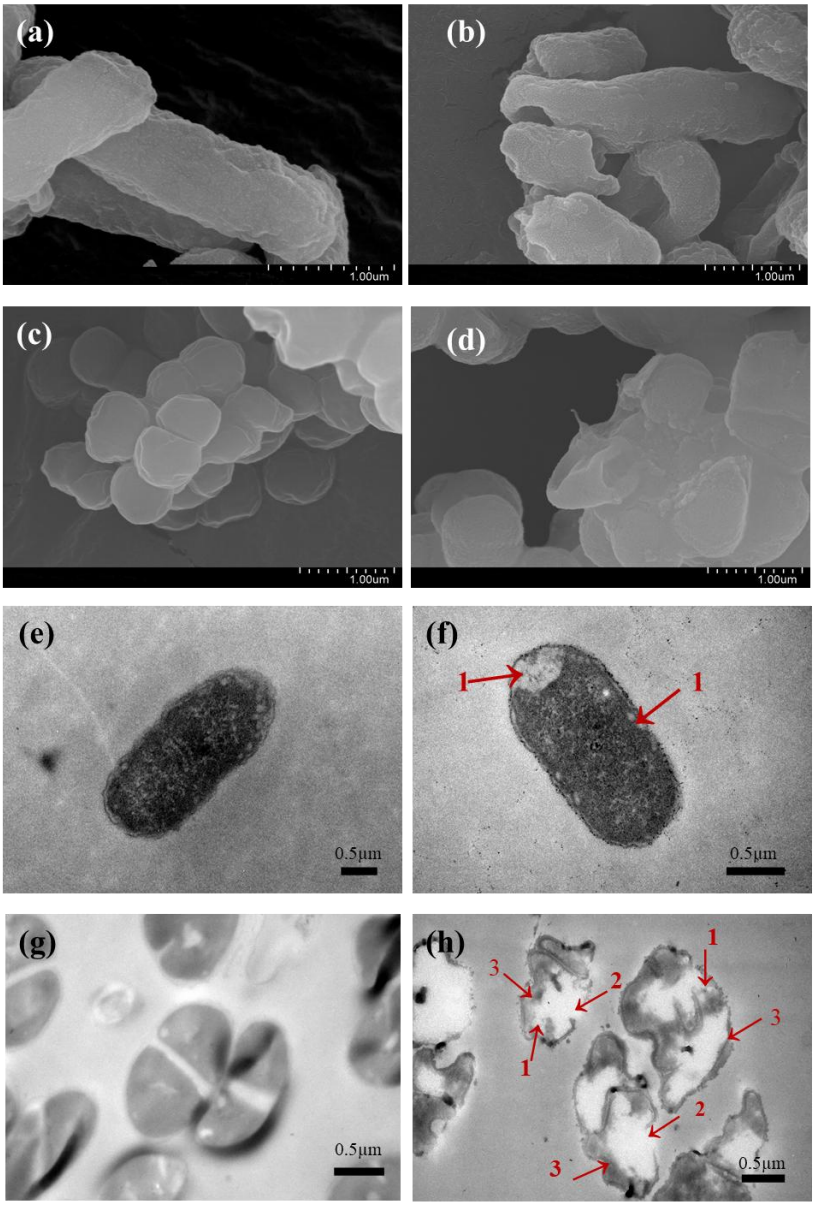

Fig S5. Effect of WGLF on cell micro-morphology and intracellular organization. (a-d): Scanning electron micrographs of (a, b) *E. coli* and (c, d) *S. aureus* treated by WGLF for 12 h. (e-h): Transmission electron micrographs of (f) *E. coli* and (h) *S. aureus* treated by WGLF for 12 h. (a) (c) (e) (g): untreated cell; (b, f): *E. coli* cells treated with WGLF at 2MIC level; (d, h): *S. aureus* cells treated with WGLF at MIC level. The leakage of cytoplasmic content and the separation of cytoplasmic membrane from the cell wall (arrows #1), discontinuity and ruptured cell surface (arrows #2) and distortion of the cell (arrows #3) were visible.

Reference

Chen L-Y, Wu J-Y, Liang J-y. 2018. Using chromatography and mass spectrometry to monitor isomerization of catechin in alkaline aqueous with thermal processing. Journal of Food Processing and Preservation.42:1-8.

CLSI. 2012. Performance standards for antimicrobial disk susceptibility tests, approved standard (7th ed.) CLSI document M02-A11. Clinical and Laboratory Standards Institute, 950 West Valley Road, Suite

2500, Wayne, Pennsylvania 19087, USA.

Flores G, Wu SB, Negrin A, Kennelly EJ. 2015. Chemical composition and antioxidant activity of seven cultivars of guava (Psidium guajava) fruits. Food chemistry.170:327-335.

Gutiérrez RM, Mitchell S, Solis RV. 2008. Psidium guajava: a review of its traditional uses, phytochemistry and pharmacology. Journal of Ethnopharmacology.117:1-27.

Gullon B, Pintado ME, Pérez-Álvarez JA, Viuda-Martos M. 2016. Assessment of polyphenolic profile and antibacterial activity of pomegranate peel (Punica granatum) flour obtained from co-product of juice extraction. Food Control.59:94-98.

Liu G, Ren G, Zhao L, Cheng L, Wang C, Sun B. 2016. Antibacterial activity and mechanism of bifidocin A against Listeria monocytogenes. Food Control. 853-816.

Ming-Zhi Z, Wei W, Li-Li J, Ping-Fang Y, Ming-Quan G. 2015. Analysis of Flavonoids in Lotus (Nelumbo nucifera) Leaves and Their Antioxidant Activity Using Macroporous Resin Chromatography Coupled with LC-MS/MS and Antioxidant Biochemical Assays. Molecules.20:10553-10565.

Ouyang W, Zhu X, Wang W, Chen XX, Chen YJ, & Cao Y. (2016). Novel skeleton sesquiterpenoids isolated from guava leaves. Natural Product Research.30:898-903.

Perumal S, Mahmud R, Ismail S. 2017. Mechanism of Action of Isolated Caffeic Acid and Epicatechin 3-gallate fromEuphorbia hirta against Pseudomonas aeruginosa. Pharmacognosy Magazine.13:S311-S315.

Rojas-Garbanzo C, Zimmermann BF, Schulze-Kaysers N, Schieber A. 2016. Characterization of phenolic and other polar compounds in peel and flesh of pink guava (Psidium guajava L. cv. ‘Criolla’) by ultra-high-performance liquid chromatography with diode array and mass spectrometric detection. Food research international.SI:445-453.

Roosild TP, Castronovo S, Healy J, Miller S, Pliotas C, Rasmussen T, Bartlett W, Conway SJ, Booth IR. 2010. Mechanism of ligand-gated potassium efflux in bacterial pathogens. Proc Natl Acad Sci U S A.107:19784-19789.

Schieber A, Hilt P, Conrad J, Beifuss U, Carle R. 2015. Elution order of quercetin glycosides from apple pomace extracts on a new HPLC stationary phase with hydrophilic endcapping. Journal of separation science.25:361-364.

Sharma A, Srivastava S. 2014. Anti-Candida activity of two-peptide bacteriocins, plantaricins (Pln E/F and J/K) and their mode of action. Fungal Biology.118:264-275.

Tang C, Xie B, Sun Z. 2017. Antibacterial activity and mechanism of B-type oligomeric procyanidins from lotus seedpod on enterotoxigenic Escherichia coli. Journal of Functional Foods.38:454-463.

Venditti A & Ukwueze SE. 2016. A possible glycosidic benzophenone with full substitution on b-ring from

psidium guajava leaves. Natural Product Research.31:739-741.

Wang C, Chang T, Yang H, Cui M. 2015. Antibacterial mechanism of lactic acid on physiological and morphological properties of Salmonella Enteritidis, Escherichia coli and Listeria monocytogenes. Food Control.47:231-236.

Xie Y, Zheng Y, Dai X, Wang Q, Cao J, Xiao J. 2015. Seasonal dynamics of total flavonoid contents and antioxidant activity of Dryopteris erythrosora. Food chemistry.186:113-118.

Xiong LG, Chen YJ, Tong JW, Huang JA, Li J, Gong YS, Liu ZH. 2017. Tea polyphenol epigallocatechin gallate inhibits Escherichia coli by increasing endogenous oxidative stress. Food chemistry. Feb 15;217:196-204.